

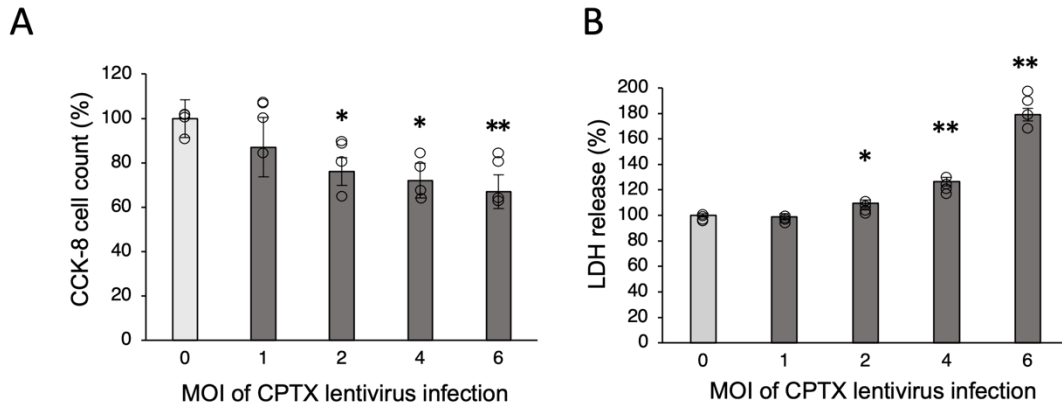
Stem Cell Reports, Volume 19

Supplemental Information

Human-induced pluripotent stem cell-derived neural stem/progenitor cell *ex vivo* gene therapy with synaptic organizer CPTX for spinal cord injury

Yusuke Saijo, Narihito Nagoshi, Momotaro Kawai, Takahiro Kitagawa, Yu Suematsu, Masahiro Ozaki, Munehisa Shinozaki, Jun Kohyama, Shinsuke Shibata, Kosei Takeuchi, Masaya Nakamura, Michisuke Yuzaki, and Hideyuki Okano

1 **Supplemental information**



2

3

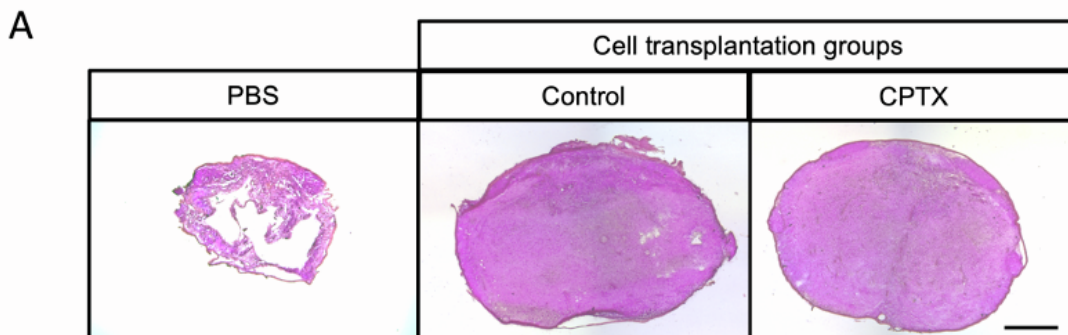
4 **Figure S1. Evaluation of lentivirus-induced cytotoxicity and cell viability**

5 (A) Measurement of neural cell counts using CCK-8 assays after lentiviral administration
6 with various doses (MOI1, 2, 4, 6), compared with negative control.

7 100.00% [8.51%]; MOI1, 86.67% [13.43%], $p = 0.26$; MOI2, 75.75% [6.29%], $p = 0.016$;
8 MOI4, 71.75% [7.76%], $p = 0.011$; MOI6, 66.77% [7.61%], $p = 0.005$; $n = 4$ each
9 independent experiments.

10 (B) LDH release from neural cells after lentiviral administration at various doses (MOI1,
11 2, 4, 6), compared with the negative control. 100.00% [1.27%]; MOI1, 98.9% [2.39%], p
12 = 0.72; MOI2, 109.43% [2.87%], $p = 0.024$; MOI4, 126.48% [3.22%], $p = 0.0009$; MOI6,
13 179.06% [4.97%], $p = 0.0005$. $n = 4$ each independent experiments.

14 Values are the mean \pm SEM. Not significant (N.S.), * $p < 0.05$, ** $p < 0.01$. Statistical
15 analyses were performed using a Mann-Whitney U-test in (A) and (B).

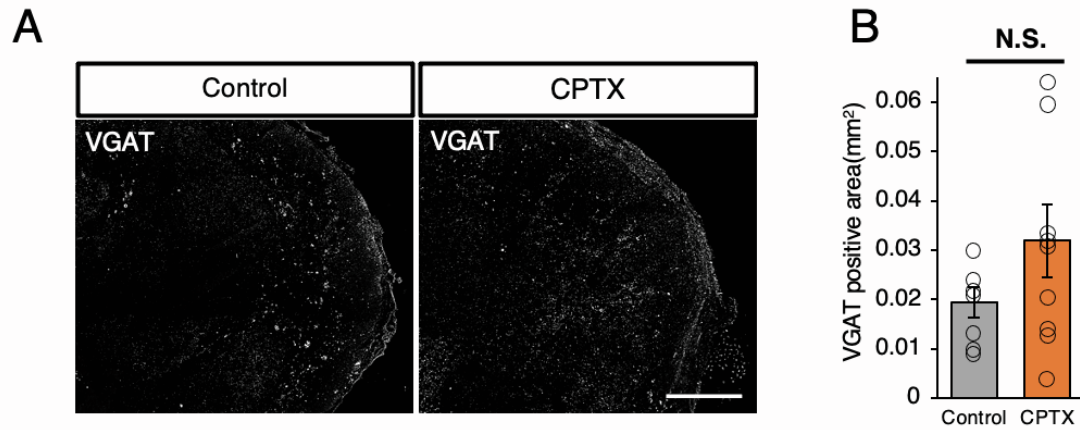


16

17 **Figure S2. H&E staining of a spinal cord sections**

18 (A) Representative images of the H&E-stained axial section at the epicenter after

19 14 weeks after SCI. PBS group (left), control group (middle), CPTX group (right). Scale
20 bar 500 μ m.



21

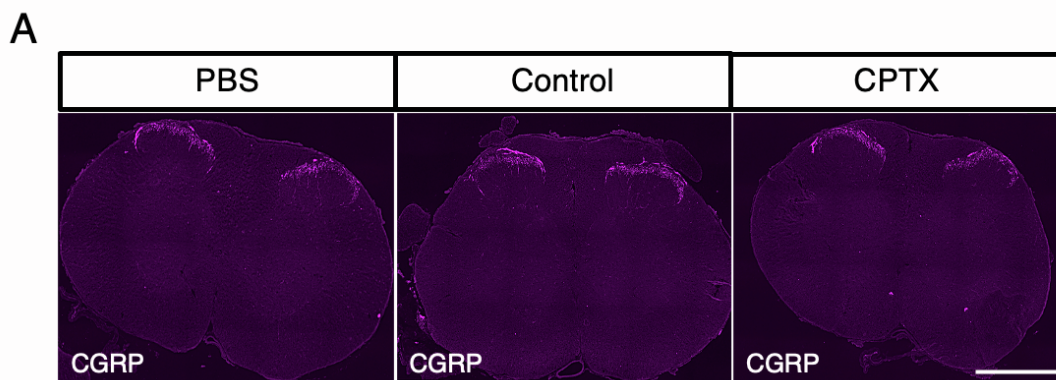
22 **Figure S3. Immunohistochemical staining with inhibitory synaptic markers**

23 (A) Representative images of VGAT (Inhibitory presynaptic marker)-positive area at
24 center of transplantation. Scale bars: 100 μ m.

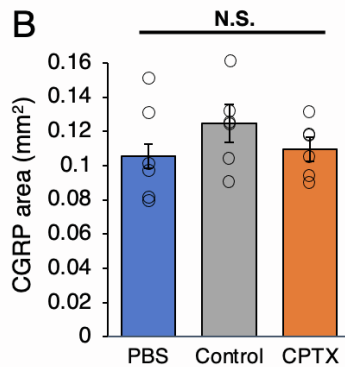
25 (B) Quantitative analysis of VGAT-positive area in axial section (control group n = 7,
26 CPTX group n = 9, p = 0.27).

27 Values are the mean \pm SEM. Not significant (N.S.), *p < 0.05, **p < 0.01. Statistical
28 analyses were performed using a Mann-Whitney U-test.

29



30



31

32 **Figure S4.** Immunohistochemical staining of calcitonin gene-related peptide (CGRP)

33 (A) Representative images of CGRP-positive area at lumbar spinal cord. Scale bars: 1
34 mm.

35 (B) Quantitative analysis of CGRP-positive area of spinal dorsal horn in three groups (n=6
36 each) PBS vs. control, $p = 0.3$, PBS vs. CPTX, $p = 0.13$, control vs CPTX, $p = 0.88$.

37 Values are the mean \pm SEM. Not significant (N.S.), * $p < 0.05$, ** $p < 0.01$. Statistical
38 analysis was performed using the Mann-Whitney U test following the Kruskal-Wallis
39 test for CGRP analysis.

40

41 **Supplemental Experimental Procedures**

42 **Lentiviral vector preparation**

43 The construction data for the CPTX were provided by Dr. Suzuki (Keio University). The
44 pLV-CAG-CPTX-His plasmid was generated using Vector Builder. Recombinant
45 lentivirus expressing CAG-CPTX-His were generated through transient transfection with
46 these plasmids: pCAG-HIVgp, pCMV-VSV-G-RSV-Rev (Miyoshi et al., 1998), and the
47 lentiviral vector plasmid. Transfection of HEK293T cells was performed as previously
48 described (Iida et al., 2017, Kojima et al., 2019). The culture supernatant containing the
49 lentivirus was concentrated using ultracentrifugation (25000 rpm for 2 hours at 4 °C). Viral
50 particles were quantified by infecting HEK293T cells with serial dilutions of the vectors,
51 followed by the measurement of the proportion of cells expressing the His-tag. The MOI
52 for hiPSC-NS/PCs was calculated based on these functional titers.

53

54 **Cell culture and lentiviral transduction**

55 The integration-free human umbilical cord-derived hiPSC line YZWJs513, which was
56 derived from a clinical-grade "human leukocyte antigen (HLA) superdonor" line
57 (Umekage et al., 2019) at the Good Manufacturing Practice (GMP)-grade cell processing
58 facility at the Center for iPS Cell Research and Application at Kyoto University (CiRA),

59 was used in this experiment. hiPSCs were produced in CiRA following previously
60 reported the differentiation protocols for NS/PCs. Cells were cultured in a floating culture
61 system. After culturing for 10 days, the cells were passaged, and infected with lentivirus.
62 Lentivirus transduction was performed as previously reported (Nori et al., 2011; Okubo et
63 al., 2018). Subsequently, the cells were cultured for an additional five days, and treated
64 with N-[N-(3,5-difluorophenacetyl)-l-ananyl]-S-phenylglycine t-butyl ester (DAPT) (10 μ M,
65 D5942, Sigma-Aldrich, St. Louis, MO, USA) for 1 day before transplantation, as
66 described in a previous study (Sugai et al., 2021).

67

68 ***In vitro* and *in vivo* His-tag detection ELISA analysis**

69 Dissociated hiPSC-NS/PCs that had been infected with lentiviruses were seeded at a
70 density of 3.5×10^5 cells/well in poly D-lysine/laminin-coated 24-well plate. After culturing
71 for three days, the supernatant of the medium was collected, and the contents were
72 determined using a His-tag ELISA Detection Kit (L00436, GenScript Biotech, USA). The
73 average concentrations in the 4 wells were calculated.

74 Tissue samples were collected from rats at 13 weeks after transplantation (control,
75 group: n = 4; CPTX group, n = 4). The entire brain of each rat was homogenized with a
76 Radio-Immunoprecipitation Assay (RIPA) buffer and centrifuged to obtain a soluble
77 fraction (15000 rpm for 30 minutes, 4 °C). The supernatant was subjected to protein
78 quantification using the Bradford method, and the protein concentration was adjusted to
79 1mg/ml. Venous blood serum was collected from the inferior vena cava prior to
80 euthanasia. The samples were left at room temperature for 30 minutes, followed by
81 centrifugation (3000 rpm for 15 minutes, 4 °C) to remove blood clots. After clot removal,
82 another centrifugation was performed (10000 rpm for 15 minutes, 4 °C), and the
83 supernatant was collected. Using the sample from the brain and venous serum, the His-
84 tag concentration was measured using a His-tag ELISA Detection Kit.

85

86 **PCR and electrophoresis for NRX SS4 detection**

87 To confirm the expression of the CPTX-binding domain (NRX SS4) in hiPSC-NS/PCs,
88 dissociated hiPSC-NS/PCs were cultured for 28 days in a serum-free medium in 12-well
89 plates coated with poly-D-lysine/laminin. Total RNA was extracted from the differentiated
90 transplanted cells using the RNeasy Micro Kit (Qiagen, Inc., Hilden, Germany), and
91 cDNA was synthesized by reverse transcription using the ReverTra Ace qPCR RT master
92 mix (Toyobo Co., Ltd., Life Science Department, Osaka, Japan). A mixture of cDNA and
93 NRXSS4 manufactured primers (Applied FASMAC) was amplified by PCR. The PCR
94 products were separated by electrophoresis on an 8% polyacrylamide gel. The primers

95 used for NRXSS4 in this study are as follows (5'-3' orientation):

96 NRX1 (Forward): tcgccattgaagaatccaatg , (Reverse): gggtgcttgctattgaagat

97 NRX2 (Forward): gacgagcccaacgccatagtaa, (Reverse): tcttgatggcagcctggctgtt

98 NRX3 (Forward): caaagaggagagaacccctg, (Reverse): ggctatttgcgcctgagtgt

99

100 **Cell viability and LDH release assay**

101 The cell toxicity of the lentivirus was measured by using a Cell Counting Kit-8 (CK04;
102 Dojindo, Kumamoto, Japan), and LDH release into the medium was measured using a
103 Cytotoxicity LDH Assay Kit-WST (CK12; Dojindo) as previously described (Hayakawa et
104 al., 2016). Briefly, hiPSC-NS/PCs were seeded in a 96-well plates at a density of 150000
105 cells per well. For the Cell Counting Kit-8 assay, lentivirus was added 48 h after cell
106 suspension and incubated for 24 h. For the LDH assay, the lentivirus was added 48 h
107 after cell suspension and incubated for 3 h. Then, cell viability and cell toxicity were
108 calculated by reference to 450 nm and 490 nm light absorbance. Each simultaneously
109 cultured well was considered as an individual sample for statistical analysis.

110

111 **Animals**

112 Adult (eight-week-old) female athymic nude rats (F344/NJcl-*rnu/rnu*, weight = 110–180
113 g, CLEA Japan, Inc., Tokyo, Japan) were used for these experiments. The rats were
114 housed randomly in groups of three or four per cage (24 × 42 × 24 cm), regardless of
115 the experimental group. They were kept on a 12/12 h light/dark cycle in an environment
116 with controlled temperature and humidity and provided ad libitum access to food and
117 water. Antibiotics (orbifloxacin; Sumitomo Dainippon Pharma Animal Health, Inc.,
118 Osaka, Japan) were administered for three days after SCI and other surgeries. All
119 experimental procedures were approved by the Experimental Animal Care Committee
120 of Keio University, School of Medicine (approval no. 13020) and were performed in
121 accordance with the Guide for the Care and Use of Laboratory Animals (National
122 Institutes of Health, Bethesda, MD). In this study, all rats were anesthetized by
123 subcutaneous injection of 0.4 mg/kg medetomidine hydrochloride, 2 mg/kg midazolam,
124 and 2.5 mg/kg butorphanol.

125 A total of 18 rats were used in each group for the in vivo experiments. The exclusion
126 criteria were established as follows: 1. Rats displaying weight-supported walking (BBB
127 score > 8) within 1 week after spinal cord injury, 2. Rats with an endpoint BBB score of
128 ≥ 19, 3. Rats that developed severe pressure sores or soft tissue infections, 4. Rats
129 among the transplanted group in which histological evaluation did not reveal HNA-
130 positive cells (transplanted cells). The composition of each group was as follows: PBS

131 (weight-supported rats: n=2, infected rats: n=1), control (infected rats: n=1, BBB \geq 19
132 rats: n=2, rats with no engrafted transplanted cells: n=2), CPTX (infected rats: n=2, rats
133 without transplanted cells: n=1).

134

135 **Surgical procedures**

136 In this study, all rats were anesthetized by subcutaneous injection of 0.4 mg/kg
137 medetomidine hydrochloride, 2 mg/kg midazolam, and 2.5 mg/kg butorphanol. Contusive
138 SCI was induced at the level of the tenth thoracic spinal vertebra using an Infinite Horizon
139 impactor (220 kdyn; Precision Systems and Instrumentation, Fair-fax Station, VA, USA)
140 with a 2 mm tip, as described previously (Scheff et al., 2003). Nine days after the injury,
141 hiPSC-NS/PCs (1×10^6 cells) were injected with a 27G metal needle using a micro
142 stereotaxic injection system (KDS310; Muromachi-Kikai Co., Ltd.). An equal volume of
143 PBS was similarly injected into PBS group rats. The injected depth was 0.4 to 1.0 mm
144 and the injection speed was 1 μ L/min. All experiments were performed in accordance
145 with the Guidelines for the Care and Use of Laboratory Animals of Keio University (Tokyo,
146 Japan, Permit Number; 13020) and The National Institutes of Health Guide for the Care
147 and Use of Laboratory Animals. All surgeries were performed under anesthesia.

148

149 **Histological analyses**

150 Thirteen weeks after transplantation, the rats were anesthetized and euthanized by
151 transcardial perfusion with glyoxal (Richter et al., 2018) followed by sequential soaking
152 overnight in 10% and 30% sucrose. Spinal cord tissues were embedded in optimal
153 cutting temperature (O.C.T.) compound (Sakura Finetechnical Co., Ltd., Tokyo, Japan)
154 and sectioned at a thickness of 16 μ m for the sagittal plane and 20 μ m for the axial plane.
155 Spinal cord sections were then immunohistochemically stained for histological analysis
156 using the following primary antibodies: mouse anti-HNA: MAB4383, Merck Millipore,
157 Burlington, MA, USA, 1:400), rabbit anti-MAP2 (AB5622, Merck Millipore, 1:500), mouse
158 anti-ELAVL 3/4 (A21271, Molecular Probes Inc., Eugene, OR, USA, 1:100), rabbit anti-
159 GFAP (16825-1-AP, Proteintech, Rosemont, IL, USA 1:2000), mouse anti-adenomatous
160 polypsis coli CC-1 (APC: OP80, Merck Millipore, 1:400), rabbit anti-Nestin (18741,
161 Immuno-Biological Laboratories, Gunma, Japan, 1:400), rabbit anti-Ki67 (NCL-Ki67p,
162 Leica Biosystems, Richmond, IL, USA, 1:2000), mouse anti-synaptophysin (14-6525-82,
163 Invitrogen, Waltham, MA, USA, 1:10000), anti-postsynaptic density 95 (PSD95: 51-6900,
164 Thermo Fisher Scientific, Waltham, MA, USA, 1:100), mouse anti-human cytoplasm
165 antibody (STEM121: Y40420, Cellartis-Takara Bio, Shiga, Japan, 1:200), goat anti-GFP
166 (600-101-215, Rockland Immunochemicals, Pottstown, PA, USA, 1:1000), rabbit anti-

167 mCherry (167453, Abcam, Cambridge, UK, 1:500), mouse anti-vesicular glutamate
168 transporter 2 (VGLUT2: S29-29, Thermo Fisher Scientific, 1:100), goat anti-vesicular
169 GABA transporter (VGAT: Af620, Frontier institute, 1:250), rabbit anti-calcitonin gene-
170 related peptide (CGRP: ab47027, Abcam, 1:400). Nuclei were stained with Hoechst
171 33258 (10 µg/ml). Spinal cord injury sites were stained with hematoxylin and eosin.
172 Sample images were obtained using a fluorescence microscope (Leica Microsystem
173 THUNDER imager Live Cell LAS X Version: 3.7.5.24914) or a confocal laser scanning
174 microscope. Analyses were performed in a customized macro using ImageJ software
175 (National Institute of Health, Bethesda, MD, USA).

176

177 **G-deleted Rabies Virus Tracing Experiment**

178 i) Generation of G-deleted rabies virus

179 The G-deleted rabies virus (RABVΔG) was generated using a method similar to that
180 previously reported (Osakada et al., 2013). The genomic plasmids required for the virus
181 creation, namely pSADΔG-mCherry, pcDNA-B19, pcDNA-B19L, pcDNA-B19G (available
182 from addgene), and B7GG cells, and BHK-EnvA cells were kindly provided by
183 Dr.F.Osakada (Nagoya University, Nagoya, Japan).The following steps were used to
184 create the RABVΔG. 1. Reconstruction of RABVΔG from the provided cDNA. 2.
185 Introduction of genes using pSADΔG-mCherry, pcDNA-B19, pcDNA-B19L, pcDNA-
186 B19G into B7GG cells and collected the supernatant. 3. Amplifying the reconstructed
187 RABVΔG in B7GG cells. 4. Infection of BHK-EnvA cells with the supernatant from step
188 3 to perform pseudotyping with EnvA. 5. Concentrate the virus by subjecting the
189 supernatant from step 4 to two rounds of ultracentrifugation. 6. Measure the titer of EnvA-
190 RABVΔG using HEK-TVA cells. These processes followed the protocol described in
191 Osakada et al., 2013, with specific conditions and materials as mentioned in the same
192 reference.

193 ii) Lentivirus production for TVA and G protein gene delivery

194 A plasmid named pBOB-synP-HTB (available from addgene) contains TVA receptor and
195 G protein expression was provided by Dr. Osakada. The gene construct includes hSyp-
196 EGFP-2A-TVA-2A-RBG. To generate the recombinant lentivirus, this plasmid was
197 transfected into HEK293 cells together with other plasmids, pCAG-HIVgp and pCMV-
198 VSV-G-RSV-Rev. Transfection of HEK293T cells was carried out as previously described
199 (Iida et al., 2017, Kojima et al., 2019).The culture supernatant containing the lentivirus
200 was concentrated through ultracentrifugation (25000 rpm for 2 hours at 4°C). Viral
201 particles were quantified by infecting HEK293T cells with serial dilutions of the vectors,
202 followed by measuring the proportion of cells expressing EGFP. The Multiplicity of

203 Infection (MOI) for hiPSC-NS/PCs was calculated based on these functional titers.
204 iii) Virus infection to hiPSC-NS/PCs and administration
205 Lentivirus containing hSyn-TVA-RVG was administered to hiPSC-NS/PCs four days prior
206 to transplantation. Specifically, in the CPTX group, the medium was changed the
207 following day, and the lentivirus inducing CPTX was administered. After transplantation
208 of these cells (1×10^6 cells), 12 weeks later, G-deleted rabies virus (titer: 1.8×10^8 vg/ml)
209 was injected bilaterally at the transplantation site (2-point injection, 750 nl per injection,
210 located 500 μ m laterally from the center of the spinal cord and at a depth of 0.4–1mm
211 from the surface). A glass syringe was used for the injections, and specific post-injection
212 procedures, waiting periods, and needle removal methods were used to prevent viral
213 leakage during administration. Immunohistochemical staining of cervical sections was
214 performed to evaluate the tracts seven days after the injections.

215

216 **Quantification of staining**

217 Immunohistochemical staining of all sections was quantified using ImageJ software.
218 Threshold values were maintained consistently across all analyses by observers who
219 were blinded to the experimental conditions and groups. Human human-specific
220 synaptophysin and VGLUT2 were quantified by capturing images at 20x magnification
221 at the center of the transplanted region and tiling them to assess the area across all axial
222 section fields. To quantify PSD95, we randomly selected one field at 63x magnification
223 from the central transplantation region (two areas per slide) and measured the area. In
224 the CPTX group, the inclusion of His-tag-positive cells within the field was required for
225 analysis. To assess synaptic formation, the contact points between the presynaptic and
226 postsynaptic markers were indirectly defined as synapses (Suzuki et al., 2020). Using
227 ImageJ software, the overlapping areas of synaptophysin and PSD95 were extracted,
228 and the number of these puncta was quantified. To account for bias, the number of
229 synaptophysin puncta was normalized. The location of RST in the G-deleted rabies virus
230 tracing experiment was verified based on previous studies (Liang et al., 2017). The
231 calculation was based on the average area of the RST on both sides.

232

233 **Motor-evoked potential experiments**

234 Electrophysiological experiments were performed using a Neuropack S1 MEB9402
235 signal processor 98 days after transplantation (n = 7 each), as described previously (Nori
236 et al., 2011). The surface of the T3 spinal cord was stimulated, and needle electrodes
237 were used to record the signal from the hind limb. An active electrode was placed in the
238 quadriceps muscle, a reference electrode was placed near the distal quadriceps muscle

239 tendon, and the ground electrode was placed on the back muscle. The stimulus
240 parameters were an intensity of 3 mA, a duration of 0.2 ms, and an interstimulus interval
241 of 1 Hz.

242

243 **Statistical analyses**

244 Statistical analyses were performed using SPSS (Japan IBM, Tokyo, Japan, Ver.
245 26.0.0.0). The normality of the distribution of data points was verified using Shapiro-Wilk
246 test. Data are reported as the mean \pm standard error of mean (SEM). Sample sizes are
247 indicated in the respective figure legends. The Mann-Whitney U-test was used for
248 comparisons between two groups *in vitro* and *in vivo* immunohistochemistry (IHC)
249 staining results. All multiple testing data were analyzed by the Kruskal-Wallis test in
250 treadmill gait, muscle weight, CGRP staining, allodynia and MEP assays. Two-way
251 repeated measures analysis of variance (ANOVA) was used for weekly BBB scoring. P
252 values < 0.05 indicate statistical significance (as * $p < 0.05$, ** $p < 0.01$).

253

254 **Supplemental References**

- 255 1. Iida, T., Iwanami, A., Sanosaka, T., Kohyama, J., Miyoshi, H., Nagoshi, N., Kashiwagi,
256 R., Toyama, Y., Matsumoto, M., Nakamura, M., and Okano, H. (2017). Whole-
257 Genome DNA Methylation Analyses Revealed Epigenetic Instability in Tumorigenic
258 Human iPS Cell-Derived Neural Stem/Progenitor Cells. *Stem Cells* 35, 1316-1327.
259 10.1002/stem.2581.
- 260 2. Kojima, K., Miyoshi, H., Nagoshi, N., Kohyama, J., Itakura, G., Kawabata, S., Ozaki,
261 M., Iida, T., Sugai, K., Ito, S., et al. (2019). Selective Ablation of Tumorigenic Cells
262 Following Human Induced Pluripotent Stem Cell-Derived Neural Stem/Progenitor
263 Cell Transplantation in Spinal Cord Injury. *Stem Cells Transl Med* 8, 260-270.
264 10.1002/sctm.18-0096.
- 265 3. Liang, H., Paxinos, G., and Watson, C. (2012). The red nucleus and the rubrospinal
266 projection in the mouse. *Brain Structure and Function* 217, 221-232.
267 10.1007/s00429-011-0348-3.
- 268 4. Miyoshi H, Blomer U, Takahashi M, Gage FH, Verma IM. Development of a self-
269 inactivating lentivirus vector. *J Virol*. 1998;(10):8150-7
- 270 5. Nori, S., Okada, Y., Yasuda, A., Tsuji, O., Takahashi, Y., Kobayashi, Y., Fujiyoshi, K.,
271 Koike, M., Uchiyama, Y., Ikeda, E., et al. (2011). Grafted human-induced pluripotent
272 stem-cell-derived neurospheres promote motor functional recovery after spinal cord
273 injury in mice. *Proc Natl Acad Sci U S A* 108, 16825-16830.
274 10.1073/pnas.1108077108.

- 275 6. Okubo, T., Nagoshi, N., Kohyama, J., Tsuji, O., Shinozaki, M., Shi-
276 bata, S., Kase, Y.,
277 Matsumoto, M., Nakamura, M., and Okano, H. (2018). Treatment with a gamma-
278 secretase inhibitor promotes functional recovery in human ipsc-
279 derived transplants
280 for chronic spinal cord injury. *Stem Cell Rep.* 11, 1416–1432.
- 281 7. Richter, K.N., Revelo, N.H., Seitz, K.J., Helm, M.S., Sarkar, D., Saleeb, R.S., D'Este,
282 E., Eberle, J., Wagner, E., Vogl, C., et al. (2018). Glyoxal as an alternative fixative to
283 formaldehyde in immunostaining and super-resolution microscopy. *EMBO J* 37, 139-
284 159. 10.15252/embj.201695709.
- 285 8. Umekage, M., Sato, Y., and Takasu, N. (2019). Overview: an iPS cell stock at CiRA.
286 *Inflamm Regen* 39, 17. 10.1186/s41232-019-0106-0.
- 287 9. Scheff, S.W., Rabchevsky, A.G., Fugaccia, I., Main, J.A., and Lump, J.E., Jr. (2003).
288 Experimental modeling of spinal cord injury: characterization of a force-defined injury
289 device. *J Neurotrauma* 20, 179-193. 10.1089/08977150360547099.
- 290 10. Sugai, K., Sumida, M., Shofuda, T., Yamaguchi, R., Tamura, T., Kohzaki, T., Abe, T.,
291 Shibata, R., Kamata, Y., Ito, S., et al. (2021). First-in-human clinical trial of
292 transplantation of iPSC-derived NS/PCs in subacute complete spinal cord injury:
293 Study protocol. *Regen Ther* 18, 321-333. 10.1016/j.reth.2021.08.005.
- 294 11. Suzuki, K., Elegheert, J., Song, I., Sasakura, H., Senkov, O., Matsuda, K.,
295 Kakegawa, W., Clayton, A.J., Chang, V.T., Ferrer-Ferrer, M., et al. (2020). A
synthetic synaptic organizer protein restores glutamatergic neuronal circuits.
Science 369. 10.1126/science.abb4853.